FEBS Letters 580 (2006) 4195–4199

Mouse stefins A1 and A2 (*Stfa1* and *Stfa2*) differentiate between papain-like endo- and exopeptidases

Marko Mihelič[a], Cory Teuscher[b], Vito Turk[a], Dušan Turk[a,*]

[a] *Department of Biochemistry and Molecular Biology, J. Stefan Institute, Jamova 39, 1000 Ljubljana, Slovenia*
[b] *Departments of Medicine and Pathology, C317 Given Medical Building, University of Vermont, Burlington, VT 05405, USA*

Received 23 April 2006; revised 13 June 2006; accepted 28 June 2006

Available online 5 July 2006

Edited by Miguel De la Rosa

Abstract **Stefin A (*Stfa*) acts as a competitive inhibitor of intracellular papain-like cysteine proteases which play important roles in normal cellular functions such as general protein turnover, antigen processing and ovarian follicular growth and maturation. In the mouse there are at least three different variants of *Stfa* (*Stfa1*, *Stfa2* and *Stfa3*). Recent genetic studies identified structural polymorphisms in *Stfa1* and *Stfa2* as candidates for *Aod1b*, a locus controlling susceptibility to day three thymectomy (D3Tx)-induced autoimmune ovarian disease (AOD). To evaluate the functional significance of these polymorphisms, recombinant allelic proteins were expressed in *Escherichia coli*, purified and characterized. The polymorphisms do not markedly alter the folding characteristics of the two proteins. *Stfa1* and *Stfa2* both act as fast and tight binding inhibitors of endopeptidases papain and cathepsins L and S, however their interaction with exopeptidases cathepsins B, C and H was several orders of magnitude weaker compared to human, porcine and bovine *Stfa*. Notwithstanding, the K_i values for the interactions of *Stfa1-b* from AOD resistant C57BL/6J mice was 10-fold higher than that of the *Stfa1-a* allele from susceptible A/J mice for papain, cathepsins B, C and H but not L and S. In contrast, the inhibitory activities of *Stfa2-a* and *Stfa2-b* were found to be roughly equivalent for all targets peptidases.**

Keywords: Stefin A; Cystatins; Cathepsin; Autoimmunity; Antigen processing; Ovarian dysgenesis

1. Introduction

The thymus is the primary site of T-cell development [1] and its removal from 3-day-old mice (day 3 thymectomy – D3Tx) leads to a loss of peripheral tolerance and the development of organ-specific autoimmune diseases during adulthood. D3Tx does not lead to autoimmune disease in all mouse strains, indicating that the development of these diseases is genetically controlled [2]. For example, A/J mice are highly susceptible to autoimmune ovarian disease (AOD) whereas C57BL/6J mice are not. Previously, using quantitative trait locus (QTL) linkage analysis we identified five regions of the mouse genome harboring loci (*Aod1–Aod5*) controlling susceptibility to AOD and its intermediate phenotypes, anti-ovarian autoantibody production, oophoritis, and atrophy [3]. Subsequently, congenic mapping revealed that *Aod1* encompassed two linked loci with opposing allelic effects on disease susceptibility (*Aod1a* and *Aod1b*) and lead to the identification of structural polymorphisms in Stefin A1 (*Stfa1*) and A2 (*Stfa2*) as candidates for *Aod1b*.

Stefins A (*Stfa*) are non-glycosylated intracellular inhibitors of cysteine cathepsins [4] including cathepsin S and L. Cathepsins S and L plays an important role in antigen processing and presentation [5] and cathepsin S has been shown to play a role in the development of D3Tx-induced autoimmune disease [6]. Additionally, cathepsins are involved in ovarian follicle growth and maturation [7]. They exhibit complex temporal and spacial expression patterns at different stages of the estrous cycle and follicular development consistent with divergent functions for specific cathepsins in follicular development, growth and rupture [8]. In contrast to human, at least three different *Stfa* variants are encoded within the mouse genome (*Stfa1*, *Stfa2*, and *Stfa3*) [9]. They share 60–65% identity in amino acid sequences and 55–60% identity when compared to human *Stfa*.

The structural polymorphisms that distinguish the C57BL/6J (*Stfa1-b* and *Stfa2-b*) and A/J (*Stfa1-a* and *Stfa2-a*) alleles may influence the folding properties and/or their affinity of binding to their target proteases. In order to evaluate the functional significance of these polymorphisms all four variants of mouse *Stfa* were expressed and their interaction constants with papain and a variety of cysteine cathepsins were determined. The alleles of *Stfa1* and *Stfa2* were essentially equivalent as functional inhibitors of several papain-like cysteine proteases; however, the *Stfa1-a* and *Stfa2-a* alleles have a detectable impact on their interaction with these proteases compared to *Stfa1-b* and *Stfa2-b*.

2. Materials and methods

2.1. Materials

Plasmids and expression strains for bacterial and yeast expression were from Novagen and Invitrogen, respectively. Restriction endonucleases and other molecular biology enzymes were from New England Biolabs. Ion-exchange and gel-filtration carriers were from Amersham Pharmacia Biotech. Fluorogenic substrates were from Bachem, other chemicals and salts used in experiments were from Serva. cDNA clones for mouse cathepsin L (clone ID: IRAKp961H028Q2) and cathepsin S (clone ID: IMAGp998M103751Q3) were obtained from RZPD (www.rzpd.de).

2.2. Cloning, expression and purification of mouse stefin A variants

The cDNA clones for mouse *Stfa1* and *Stfa2* were amplified by polymerase chain reaction (PCR). The PCR products were digested with *Nde*I and *Bam*HI and subcloned into pET-3a or pET-11a expression vector.

*Corresponding author. Fax: +386 1 477 3984.
E-mail address: dusan.turk@ijs.si (D. Turk).

0014-5793/$32.00
doi:10.1016/j.febslet.2006.06.076

Escherichia coli strain BL21DE3 pLysS was used for expression. Cells transformed with recombinant plasmids were grown at 37 °C in Luria-Bertani (LB) medium, containing 100 μg/ml ampicillin and 50 μg/ml chloramphenicol to OD600 0.6. Expression was induced by addition of isopropyl β-D-thiogalactoside (IPTG) to a final concentration of 0.4 mM. After 1–4 h of induction, the cells were harvested by centrifugation and resuspended in the ice-cold lysis buffer (50 mM Tris–HCl, 0.1 M NaCl, 1 mM EDTA, pH 8). Cell disruption was achieved by freezing and thawing of the cell suspension and by sonification. Nucleic acids were precipitated by the addition of 5% solution of polyethyleneimine to a final concentration of 0.1% and removed together with the insoluble fractions of bacterial cells by centrifugation. Clear cytosolic fraction was concentrated and loaded onto a Superdex G-75 gel filtration column equilibrated in 30 mM Tris–HCl, 0.3 M NaCl, pH 8.0. Eluted fractions were analyzed by sodium dodecyl sulfate–polyacrylamide gel electrophoresis (SDS–PAGE). Fractions containing recombinant protein were collected, dialyzed against 30 mM Tris–HCl, pH 8, and applied onto a SP-Sepharose Fast Flow column equilibrated with the same buffer. The elution was carried out with a linear gradient of NaCl (0–0.5 M) in the starting buffer. Fractions containing pure protein, as judged by SDS–PAGE analysis, were pooled and concentrated.

2.3. Cloning, expression and purification of mouse cathepsins L and S

The cDNA region encoding mouse procathepsins L and S were amplified by PCR. Amplified DNA products were digested with *Xho*I and *Not*I and ligated into pPIC9 expression plasmid. The recombinant plasmids were subsequently linearized with *Sal*I and electroporated into *Pichia pastoris* strain GS115 using Gene Pulser (Bio-Rad). The recombinant clones of *P. pastoris* were selected on MD agar plates. The integration of recombinant plasmid into the genome of *P. pastoris* was additionally examined by the yeast colony PCR as described in [10]. 40 recombinant clones were tested for protein production using small 50 ml bioreactors (TPP). The clone with the highest level of protein production, as judged by the SDS–PAGE analysis, was selected for large-scale expression.

Mature mouse cathepsin S was purified from the expression media using ion-exchange chromatography step on SP-Sepharose Fast Flow equilibrated in 30 mM sodium acetate, 1 mM EDTA, pH 5.5. Proteins were eluted using linear gradient of NaCl (0–0.5 M) in the starting buffer. Fractions containing cathepsin S were additionally purified on Superdex G-75 gel filtration column.

Crude expression media containing mouse procathepsin L was dialyzed against 30 mM Tris–HCl, 1 mM EDTA, pH 7.5 buffer and loaded onto a Q-Sepharose Fast Flow column. Procathepsin L containing fractions were eluted with equilibration buffer containing 0.5 M NaCl, dialyzed against 30 mM sodium acetate, 1 mM EDTA, 2 mM DTT, pH 5, and applied onto SP-Sepharose Fast Flow ion exchange column equilibrated with the same buffer. Pure fractions of mature cathepsin L were eluted using equilibration buffer containing 0.3 M NaCl.

2.4. Circular dichroism spectroscopy

The protein was dissolved in the 10 mM phosphate buffer, pH 5.5, at concentration of 0.5 mg/ml. The far-UV CD spectra were measured at room temperature (22 °C) on the Aviv 60DS spectrometer (Piscataway, NJ, USA). Data points were recorded from 250 to 190 nm using 1 nm interval and a cell path length of 0.1 cm. The bandwidth was set to 1 nm.

2.5. Kinetics of inhibition

In all kinetic experiments, papain, cathepsin S, cathepsin H and cathepsin B were assayed using 0.1 M phosphate buffer, pH 6.0, containing 3 mM DTT and 1 mM EDTA, whereas for cathepsin C, 100 mM NaCl was added into assay buffer. Cathepsins L was assayed in 0.1 M acetate buffer, pH 5.5, containing 3 mM DTT and 1 mM EDTA. The active concentration of enzymes was determined by active site titration using cysteine protease inhibitor E-64 or human recombinant *Stfa* pretitrated with papain.

All inhibition experiments were performed under the pseudo first-order conditions with inhibitor concentration at least 10-fold higher than the enzyme concentrations and less than 10% of substrate was hydrolyzed during these experiments. *Stfa* variants were in various concentrations mixed with substrate solution dissolved in the appropriate buffer in the fluorometric cuvette. The reaction was initiated by the addition of enzyme in a negligible volume. Constant concentrations of papain (50 pM), cathepsin L (30 pM), cathepsin S (60 pM), cathepsin C (100 pM), cathepsin H (300 pM) and cathepsin B (100 pM) and substrates (10 μM Z-Phe-Arg-MCA for papain, cathepsin L, cathepsin B and cathepsin S and 10 μM Z-Arg-MCA for cathepsin H) were used throughout the measurements. The progress curves were monitored at excitation and emission wavelengths of 370 and 460 nm, respectively, using a C-61 fluorimeter (Photon Technology International).

In all cases, typical biphasic curves were observed and were analyzed by the least-square fitting to the appropriate equation [11]. Linear dependence of pseudo first-order rate constant against the inhibitor concentration was observed for all enzyme-inhibitor pairs. Apparent association rate constants, k_{ass}, were obtained from these plots and were additionally corrected for substrate competition using adequate K_m values. K_{diss} were obtained from the intercepts of slopes with the ordinate and K_i values were calculated from the obtained k_{ass} and k_{diss} values. If the intercept was too close to the origin of the axis, precluding an accurate determination of k_{diss}, K_i values were determined by the equilibrium method [12]. In these cases, k_{diss} values were calculated from $k_{diss} = K_i/k_{ass}$.

3. Results and discussion

3.1. Location of polymorphisms within Stfa1 and Stfa2 alleles

The sequences of the C57BL/6J and A/J *Stfa1* and *Stfa2* alleles are homologous to human *Stfa*. They posses all secondary structural elements constituting the fold of stefins, the N-terminal helix and four stranded beta sheets, as well as the structural features crucial for effective binding to the active sites of their target proteases (Fig. 1, using human *Stfa* nomenclature), the N-terminal trunk, the first hairpin loop with the characteristics of QVVAG motif (where the first V47 can be replaced by A and the A49 by Q) and the second hairpin loop [13,14].

The N-terminal trunk of *Stfa1-a* is one amino acid shorter than *Stfa1-b*, whereas the *Stfa2-a* and *Stfa2-b* alleles both possess a seven residue long N-terminal extension when compared to human *Stfa*. As can be seen from the theoretical models of *Stfa1* and *Stfa2*, most variable positions are located in the regions distant to the active site cleft (Fig. 2). Among the variable positions only positions 2 (S2 *Stfa1-b* – M2 *Stfa1-a* substitution) and 3 (L3 *Stfa1-b* – Y3 *Stfa1-a*, I3 *Stfa2-b* – M3 *Stfa2-a* substitution) at the N-terminal trunk and position 47 within the first hairpin loop, where V47 has been changed to A in *Stfa1-a*, are contributing to the direct interactions with the active site of the target enzymes. This short analysis suggests that there are likely no significant differences in folding properties between the predominant and variable forms of mouse *Stfa*, whereas a possibility exists that there are differences in their binding affinities primarily due to variability of the N-terminal trunk region.

3.2. Folding of mouse Stfa1 and Stfa2

Stfa1 and *Stfa2* from C57BL/6J and A/J mice were expressed in *E. coli* using a vector for cytosolic expression. Formation of appropriately folded structures was verified by assessing their far UV-CD spectra (Fig. 3). The spectra of *Stfa2* markedly differ from the spectra of *Stfa1* in that they exhibit an increased negative molecular ellipticity between 210 and 220 nm and decreased molecular ellipticity at lower wavelengths. This difference is indicative of an increase in disordered structure which is presumably due to the elongated N-terminal trunk of *Stfa2*. Aside from this difference, the spectra for *Stfa1* and *Stfa2* are similar to human *Stfa* spectra. Furthermore, the spectra

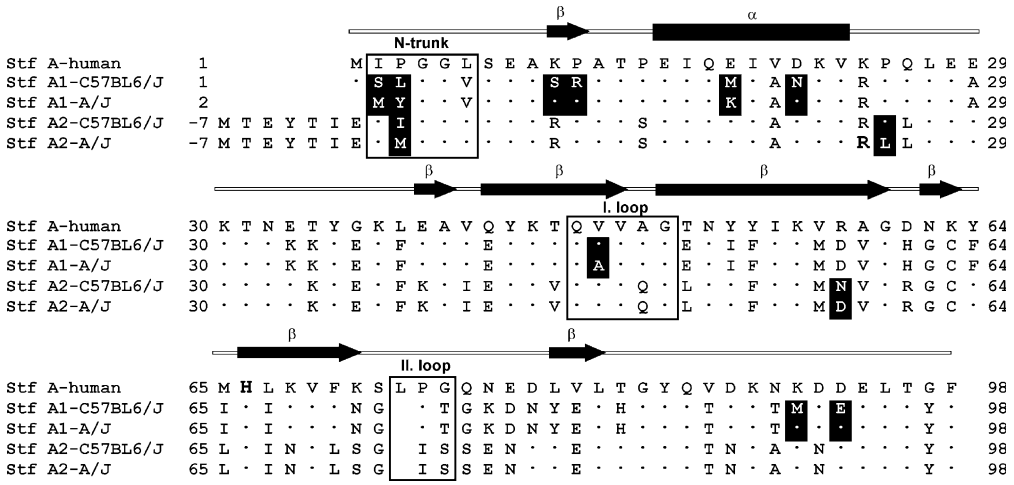

Fig. 1. Alignment of amino acid sequences of human *Stfa* and mouse C57BL/6J and A/J *Stfa1* and *Stfa2*. The location of *Stfa1* and *Stfa2* polymorphisms from A/J strain of mice are shaded. Secondary structure elements and N-terminal trunk, the first and the second hairpin loops are marked.

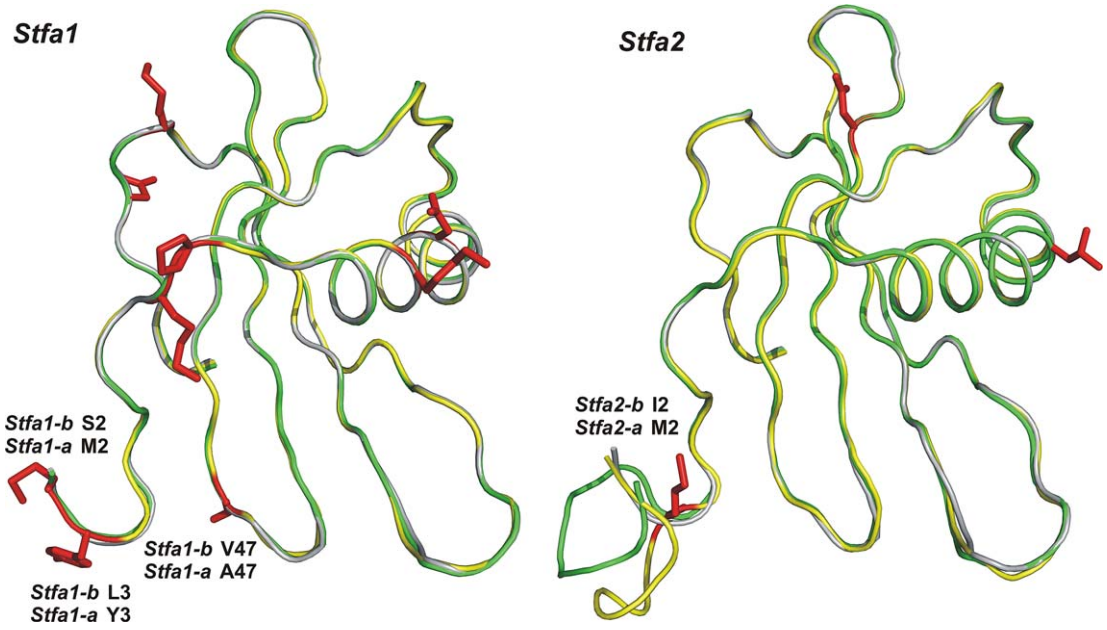

Fig. 2. Comparison of three-dimensional models of mouse C57BL/6J (*Stfa-b*) and A/J (*Stfa-a*) *Stfa1* (left) and *Stfa2* (right) with human *Stfa*. Models of mouse *Stfa* variants were produced by homology modeling approach using crystal structure of human *Stfa* as a template [14]. Main chain worm model of human *Stfa* is shown in gray, whereas main chains of mouse stefin models are shown in yellow and green, respectively. The amino acid polymorphisms from A/J strain are presented with red sticks. Polymorphisms located at the protease interaction regions are labeled.

for the *Stfa1* alleles and the *Stfa2* alleles are identical indicating that the polymorphisms do not markedly alter the folding characteristics of the two inhibitors.

3.3. Inhibitory properties of mouse Stfa1 and Stfa2

To explore the inhibitory properties of *Stfa1* and *Stfa2* their interaction constants with several different target proteases, cathepsins L, S, H, B, C and papain were determined (Table 1). Both *Stfa1* and *Stfa2* were found to act as fast and tight binding inhibitors of endopeptidases cathepsins L and S and papain, although the inhibition constants are slightly higher than those reported for *Stfa* from other species [15–17]. In contrast more pronounced differences were observed in the interaction of *Stfa1* and *Stfa2* with exopeptidases.

Interactions of cystatins with these exopeptidases are in general weaker, but still within the low nanomolar range [15–18]. Exopeptidases cathepsins B, H and C poses unique structural features that restrain binding of substrates and inhibitors to the parts of the active site cleft [19]. These features compete with inhibitors for binding into the same sites on the surface of target proteases. According to the model of cystatin-papain-like protease complex N-terminal trunk competes with the features of aminopeptidases: the mini-chain of cathepsin H [20] and the exclusion domain residues of cathepsin C [21], whereas the second hairpin loop competes for binding with the occluding loop of carboxypeptidase cathepsin B [22].

In contrast to the K_i values for human, porcine and bovine *Stfa* as reported previously, inhibition of exopeptidases by

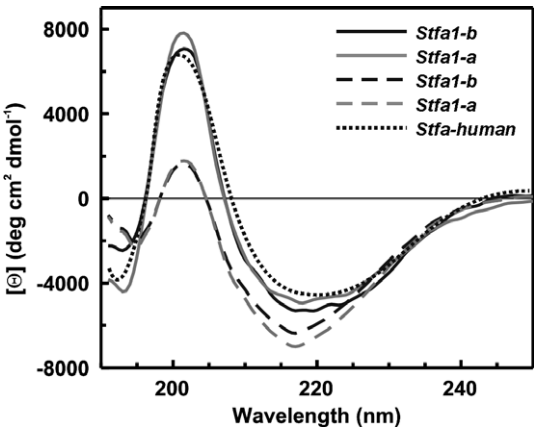

Fig. 3. Far ultraviolet spectra of human *Stfa* and mouse C57BL/6J and A/J *Stfa1* and *Stfa2*.

mouse *Stfa1* and *Stfa2* is several orders of magnitude weaker. In general mouse *Stfa2* was a better inhibitor of mouse cathepsin B, human cathepsins C and porcine cathepsin H than mouse *Stfa1*. These data suggest that mouse *Stfa1* is not a particularly good inhibitor of papain-like exopeptidases (K_i values are in micromolar range), whereas *Stfa2* inhibits cathepsins H and C in the nanomolar range and cathepsin B in the micromolar range.

Mutational analysis of the second binding loop residues of human *Stfa* showed that the most significant contribution to the inhibitory activity is provided by residue L73 building hydrophobic interactions with the conserved side chain of W177 papain located at the bottom of S1′ subsite [23]. Its mutation to glycine decreased the affinity for papain and cathepsins L and B by 300-fold, 10-fold and 4000-fold, respectively. These results confirm that tight interactions within the second hairpin loop are more important for interaction with the exopeptidase cathepsin B than for the endopeptidases tested. From these data we can conclude that missing L73 in the sequences of mouse *Stfa1* and *Stfa2* variants is likely the cause for weaker inhibition of exopeptidases.

The *Stfa1* and *Stfa2* polymorphism have a detectable effect on their interactions with endopeptidases. The K_i values for the interaction of papain with *Stfa1-b* is 10-fold higher than that of *Stfa1-a*. However, no significant differences between the alleles were observed for their interactions with mouse cathepsins L and S. Analysis of the interactions of *Stfa1* and *Stfa2* alleles with exopeptidases also reveal differences in the inhibitory properties of alleles. The inhibitory activity of *Stfa1-a* which is shorter by a single amino acid at the N-terminal trunk for papain, cathepsin H, B and C was ~10-times lower than that of *Stfa1-b*. This difference in activity is probably due to the difference in the length of the N-terminal trunk of the two alleles. Truncation of the N-terminal M residue does not affect the inhibitory properties of human *Stfa*, while truncation of the first two amino acid residues reduces affinities for papain and cathepsins L and B [17]. The inhibitory activity of *Stfa2-a* and *Stfa2-b* for exopeptidases was found to be roughly equivalent.

Taken together, we were unable to detect any major differences in the inhibitory activity of the C57BL/6J and A/J *Stfa1* and *Stfa2* alleles for cathepsins L and S, the primary endopeptidases required for antigen processing [5], or in the inhibitory activity of the *Stfa2-a* and *Stfa2-b* for cathepsins B, C and H.

Table 1
Kinetic and equilibrium data for the interaction between C57BL/6J and A/J *Stfa1* and *Stfa2* and papain and cathepsins L, S, B, H and S

Enzyme	Inhibitor	$10^{-6} \times k_{ass}$ (M^{-1} s^{-1})	$10^{4} \times k_{diss}$ (s^{-1})	K_i (nM)	Inhibitor	K_i (nM)
Papain	Stefin A1 C57BL/6J	2.7 ± 0.14	225 ± 16.0	8.36 ± 0.390	Human stefin A	0.019
	Stefin A1 A/J	ND	ND	87.20 ± 5.030	Porcine stefin A	0.174
	Stefin A2 C57BL/6J	4.5 ± 0.34	16.2 ± 3.9	0.361 ± 0.082		
	Stefin A2 A/J	4.2 ± 0.28	5.5 ± 0.8	0.130 ± 0.016		
Cathepsin L	Stefin A1 C57BL/6J	8.7 ± 0.88	13.6 ± 3.68	0.156 ± 0.029	Human stefin A	0.31
	Stefin A1 A/J	7.6 ± 0.66	9.8 ± 1.34	0.129 ± 0.014	Porcine stefin A	0.02
	Stefin A2 C57BL/6J	2.7 ± 0.19	2.8 ± 1.64	0.104 ± 0.061	Bovine stefin A	0.029
	Stefin A2 A/J	2.4 ± 0.10	2.4 ± 0.10	0.102 ± 0.010		
Cathepsin S	Stefin A1 C57BL/6J	8.0 ± 0.56	9.6 ± 0.87	0.120 ± 0.069	Porcine stefin A	0.053
	Stefin A1 A/J	7.8 ± 0.34	5.5 ± 0.25	0.071 ± 0.008		
	Stefin A2 C57BL/6J	7.8 ± 0.24	6.3 ± 1.03	0.081 ± 0.013		
	Stefin A2 A/J	5.6 ± 0.31	6.6 ± 0.42	0.118 ± 0.023		
Cathepsin H	Stefin A1 C57BL/6J	ND	ND	110.9 ± 1.9	Human stefin A	1.3
	Stefin A1 A/J	ND	ND	2400 ± 340	Porcine stefin A	0.069
	Stefin A2 C57BL/6J	ND	ND	18.9 ± 0.3	Bovine stefin A	0.44
	Stefin A2 A/J	ND	ND	43.9 ± 2.0		
Cathepsin B	Stefin A1 C57BL/6J	ND	ND	6108 ± 1675	Porcine stefin A	2
	Stefin A1 A/J	ND	ND	>10000	Bovine stefin A	1.79
	Stefin A2 C57BL/6J	ND	ND	1853 ± 124		
	Stefin A2 A/J	ND	ND	2348 ± 130		
Cathepsin C	Stefin A1 C57BL/6J	ND	ND	144.0 ± 14.2	Human stefin A	1.1
	Stefin A1 A/J	ND	ND	5340 ± 920		
	Stefin A2 C57BL/6J	ND	ND	187.1 ± 23.3		
	Stefin A2 A/J	ND	ND	51 ± 4,3		

The interaction constants for human, porcine and bovine *Stfa* are from [15–18].

In contrast the inhibitory activity of *Stfa1-a* was significantly lower than that of *Stfa1-b* for cathepsins B, C and H, which function to trim the amino- and carboxy-terminal ends of peptides either before or after binding to major histocompatibility (MHC) class II molecules [5]. This difference in activity could impact the level and nature of antigen specific peptide-class II complexes on the surface of antigen presenting cells thereby selectively altering T cell responses in D3Tx mice in favor of either susceptibility or resistance to AOD. In addition to their role in antigen processing, one or more of cathepsins B, C and H has been implicated in a variety of cellular functions directly relevant to D3Tx-induced AOD including the regulation of apoptosis in T and B-cells [24] and in ovarian follicle growth and maturation [7,8]. Consequently potential differences in the expression profiles of inhibitors as well as target proteases should be examined in both inbred strains of mice. Given the complex temporal and spatial expression patterns of cathepsins in both the immune system and the target organ our results warrant further investigation into the role the C57BL/6J and A/J *Stfa1* alleles in the genetic control of susceptibility to D3Tx-induced AOD.

We have shown that mouse *Stfa1* and *Stfa2* act as fast and tight binding inhibitors of papain-like endopeptidases. Surprisingly they are significantly less effective against papain-like cysteine exopeptidases than human, porcine and bovine *Stfa*, suggesting that in mice *Stfa* variants are involved predominantly in the regulation of endopeptidase activity of cysteine cathepsins. Since cysteine cathepsins play a crucial role in the antigen presentation processes, these findings indicate that the interactions between *Stfa* and cathepsins contribute to the species dependent diversity of the endosomal compartments including those involved in immune response.

Acknowledgments: We thank Dr. Igor Stern, M.Sc. Dejan Caglic and Ivica Klemencic for providing us with cathepsins C, B and cathepsin H. This work was supported by the Slovenian Research Agency and by National Institutes of Health Grants AI41747 (to C.T.).

References

[1] Bhandoola, A. and Sambandam, A. (2006) From stem cell to T cell: one route or many? Nat. Rev. Immunol. 6, 117–126.
[2] Tung, K.S.K., Setiady, Y.Y., Samy, E.T., Lewis, J. and Teuscher, C. (2005) Autoimmune ovarian disease in day 3-thymectomized mice: the neonatal time window, antigen specificity of disease suppression and genetic control. CTMI 293, 209–247.
[3] Roper, R.J., McAllister, R.D., Biggins, J.E., Michael, S.D., Min, S.H., Tung, K.S., Call, S.B., Gao, J. and Teuscher, C. (2003) Aod1 controlling day 3 thymectomy-induced autoimmune ovarian dysgenesis in mice encompasses two linked quantitative trait loci with opposing allelic effects on disease susceptibility. J. Immunol. 170, 5886–5891.
[4] Barrett, A.J., Rawlings, N.D., Davies, M.E., Machleidt, W., Salvesen, G. and Turk, V. (1986) in: Proteinase Inhibitors (Barrett, A.J. and Salvesen, G., Eds.), pp. 515–569, Elsevier, Amsterdam.
[5] Chapman, H.A. (2006) Endosomal proteases in antigen presentation. Curr. Opin. Immunol. 18, 78–84.
[6] Saegusa, K., Ishimaru, N., Yangi, K., Arakaki, R., Ogawa, K., Saito, I., Katanuma, N. and Hayashi, Y. (2002) Cathepsin S inhibitor prevents autoantigen presentation and autoimmunity. J. Clin. Invest. 110, 361–369.
[7] Carnevali, O., Cionna, C., Lubzens, E. and Maradonna, F. (2006) Role of cathepsins in ovarian follicle growth and maturation. Gen. Comp. Endocrinol. 146, 195–203.
[8] Oksjoki, S., Soderstrom, M., Vuorio, E. and Anttila, L. (2001) Differential expression patterns of cathepsins B, H, K, L and S in the mouse ovary. Mol. Hum. Reprod. 7, 27–34.
[9] Tsui, F.W., Tsui, H.W., Mok, S., Mlinaric, I., Copeland, N.G., Gilbert, D.J., Jenkins, N.A. and Siminovitch, K.A. (1993) Molecular characterization and mapping of murine genes encoding three members of the stefin family of cysteine proteinase inhibitors. Genomics 15, 507–514.
[10] Linder, S., Schliwa, M. and Kube-Granderath, E. (1996) Direct PCR screening of *Pichia pastoris* clones. BioTechniques 20, 980–982.
[11] Morrison, J.F. (1982) The slow-binding and slow, tight binding inhibition of enzyme catalyzed reactions. Trends Biochem. Sci. 7, 102–105.
[12] Greco, W.R. and Hakala, M.T. (1979) Evaluation of methods for estimating the dissociation constant of tight binding enzyme inhibitors. J. Biol. Chem. 254, 12104–12109.
[13] Stubbs, M.T., Laber, B., Bode, W., Huber, R., Jerala, R., Lenarcic, B. and Turk, V. (1990) The refined crystal structure of recombinant human stefin B in complex with the cysteine proteinase papain: a novel type of proteinase inhibitor interaction. EMBO J. 9, 1939–1947.
[14] Jenko, S., Dolenc, I., Guncar, G., Dobersek, A., Podobnik, M. and Turk, D. (2003) Crystal structure of stefin A in complex with cathepsin H: N terminal residues of inhibitors can adapt to the active sites of endo- and exopeptidases. J. Mol. Biol. 326, 875–885.
[15] Lenarcic, B., Krizaj, I., Zunec, P. and Turk, V. (1996) Differences in specificity for the interactions of stefins A, B and D with cysteine proteinases. FEBS Lett. 21, 113–118.
[16] Turk, B., Ritonja, A., Bjork, I., Stoka, V., Dolenc, I. and Turk, V. (1995) Identification of bovine stefin A, a novel protein inhibitor of cysteine proteinases. FEBS Lett. 360, 101–105.
[17] Estrada, S., Pavlova, A. and Bjork, I. (1999) The contribution of N-terminal region residues of cystatin A (stefin A) to the affinity and kinetics of inhibition of papain, cathepsin B, and cathepsin L. Biochemistry 38, 7339–7345.
[18] Dahl, S.W., Halkier, T., Lauritzen, C., Dolenc, I., Pedersen, J., Turk, V. and Turk, B. (2001) Human recombinant pro-dipeptidyl peptidase I (cathepsin C) can be activated by cathepsins L and S but not by autocatalytic processing. Biochemistry 40, 1671–1678.
[19] Turk, D. and Guncar, G. (2003) Lysosomal cysteine proteases (cathepsins): promising drug targets. Acta. Crystallogr. D Biol. Crystallogr. 59, 203–213.
[20] Guncar, G., Podobnik, M., Pungercar, J., Strukelj, B., Turk, V. and Turk, D. (1998) Crystal structure of porcine cathepsin H determined at 2.1 A resolution: location of the mini-chain C-terminal carboxyl group defines cathepsin H aminopeptidase function. Structure 15, 51–61.
[21] Turk, D., Janjic, V., Stern, I., Podobnik, M., Lamba, D., Dahl, S.W., Lauritzen, C., Pedersen, J., Turk, V. and Turk, B. (2001) Structure of human dipeptidyl peptidase I (cathepsin C): exclusion domain added to an endopeptidase framework creates the machine for activation of granular serine proteases. EMBO J. 20, 6570–6582.
[22] Musil, D., Zucic, D., Turk, D., Engh, R.A., Mayr, I., Huber, R., Popovic, T., Turk, V., Towatari, T. and Katunuma, N. (1991) The refined 2.15 A X-ray crystal structure of human liver cathepsin B: the structural basis for its specificity. EMBO J. 10, 2321–2330.
[23] Pavlova, A. and Bjork, I. (2002) The role of the second binding loop of the cysteine protease inhibitor, cystatin A (stefin A), in stabilizing complexes with target proteases is exerted predominantly by Leu73. Eur. J. Biochem. 269, 5649–5658.
[24] Chwieralski, C.E., Welte, T. and Buhling, F. (2006) Cathepsin-regulated apoptosis. Apoptosis 11, 143–149.